HHS Public Access

Author manuscript

Biomaterials. Author manuscript; available in PMC 2020 November 01.

Published in final edited form as:

Biomaterials. 2019 November ; 220: 119403. doi:10.1016/j.biomaterials.2019.119403.

IFN-γ-tethered hydrogels enhance mesenchymal stem cell-based immunomodulation and promote tissue repair

José R. García[1,2], **Miguel Quirós**[3], **Woojin M. Han**[1,2], **Monique N. O'Leary**[3], **George N. Cox**[4], **Asma Nusrat**[3], **Andrés J. García**[1,2,*]

[1]Woodruff School of Mechanical Engineering, Georgia Institute of Technology, Atlanta GA, USA

[2]Petit Institute for Bioengineering and Biosciences, Georgia Institute of Technology, Atlanta GA, USA

[3]Department of Pathology, University of Michigan, Ann Arbor, MI, USA

[4]Bolder BioTechnology, Inc., Boulder, CO, USA

Abstract

Because of their immunomodulatory activities, human mesenchymal stem cells (hMSCs) are being explored to treat a variety of chronic conditions such as inflammatory bowel disorders and graft-vs-host disease. Treating hMSCs with IFN-γ prior to administration augments these immunomodulatory properties; however, this *ex vivo* treatment limits the broad applicability of this therapy due to technical and regulatory issues. In this study, we engineered an injectable synthetic hydrogel with tethered recombinant IFN-γ that activates encapsulated hMSCs to increase their immunomodulatory functions and avoids the need for *ex vivo* manipulation. Tethering IFN-γ to the hydrogel increases retention of IFN-γ within the biomaterial while preserving its biological activity. hMSCs encapsulated within hydrogels with tethered IFN-γ exhibited significant differences in cytokine secretion and showed a potent ability to halt activated T-cell proliferation and monocyte-derived dendritic cell differentiation compared to hMSCs that were pre-treated with IFN-γ and untreated hMSCs. Importantly, hMSCs encapsulated within hydrogels with tethered IFN-γ accelerated healing of colonic mucosal wounds in both immunocompromised and immunocompetent mice. This novel approach for licensing hMSCs with IFN-γ may enhance the clinical translation and efficacy of hMSC-based therapies.

*corresponding author: andres.garcia@me.gatech.edu.

Author contributions: J.R.G., M.Q., A.N. and A.J.G designed the research, analyzed the data and wrote the paper; J.R.G., M.Q., and A.J.G performed the research, analyzed the data and reviewed the manuscript. M.N.O. performed the wounding experiments, and W.H. carried out the Western blotting. G.N.C. provided recombinant cys-IFN-γ, and provided suggestions on experiments and manuscript.

Competing interests: J.R.F., M.Q., M.N.O, A.N., and A.J.G. have no conflicts to declare. G.N.C. is an employee of Bolder BioTechnology and has a financial interest in the company. G.N.C. is an inventor on patents related to cys-IFN-γ proteins.

Data and Materials availability: All materials and cells are available either commercially or upon request.

Introduction

Human mesenchymal stem cells (hMSCs) are multipotent stromal cells that, in addition to having the ability to differentiate into cell types that produce distinct tissues (e.g., bone, cartilage and fat), exhibit potent immunomodulatory activities and are being evaluated in a myriad of clinical trials for treating autoimmune and chronic inflammatory diseases [1–5]. Co-culturing hMSCs with activated T-cells or monocytes leads to reduced proliferation of T-cells and inhibition of monocyte-derived dendritic cell differentiation, respectively [6, 7]. hMSCs also have powerful inhibitory effects on other immune cell types ranging from natural killer cells to B-cells [8, 9]. Importantly, hMSC delivery ameliorates the effects of diverse autoimmune diseases in pre-clinical models of graft-vs-host disease (GvHD), colitis, and autoimmune encephalomyelitis [10–13]. Based on promising results in pre-clinical models, hMSCs have been evaluated in clinical trials for treating Crohn's disease as well as steroid-refractory acute GvHD, but with varying levels of success. In a phase II clinical study of refractory Crohn's disease, although the overall disease score was significantly reduced with administration of hMSCs, patient improvement was only noted in 7 of 15 patients [14]. Le Blanc and colleagues found that out of 55 patients having severe acute GvHD that received an infusion of hMSCs, 30 (55%) had a complete response while the other 25 had either a partial or no response to hMSC therapy [15]. Overall, these studies support the notion that hMSC therapy ameliorates autoimmune diseases, but the effect is only seen in approximately half of patients, leaving vast room for improvement [16, 17].

In order to fully elicit their immunomodulatory effects, hMSCs must be activated with pro-inflammatory stimuli, specifically interferon-gamma (IFN-γ), in a process termed 'licensing' [18, 19]. Either co-culturing hMSCs with IFN-γ-deficient immune cells or using antibodies to neutralize IFN-γ results in loss of hMSC immunomodulatory actions [20, 21]. Once licensed with IFN-γ, hMSCs elicit their immunomodulatory effects by the upregulation of immunoactive factors including indoleamine 2,3-dixygenase (IDO), programmed death ligand-1 (PD-L1), prostaglandin E2 (PGE2), CCL8, CXCL9 and CXCL10 among many others [22, 23]. Importantly, the timing and duration of licensing are crucial, and licensing hMSCs prior to co-culture or use *in vivo* enhances their immunomodulatory capabilities [24]. Licensing hMSCs with IFN-γ prior to co-culture with activated T-cells results in both inhibited T-cell proliferation and T-cell effector functions, whereas hMSCs that were not licensed prior to co-culture only inhibited T-cell proliferation [25]. Furthermore, licensing hMSCs prior to infusion into mice with GvHD results in enhanced hMSC-based suppression of GvHD compared to that of control un-licensed hMSCs [20]. Duijvestein et al also showed that delivering pre-licensed hMSCs significantly reduced the severity of experimental colitis in mice compared to un-licensed hMSCs [26].

Although *ex vivo* licensing of hMSCs is therapeutically effective, significant technical, regulatory, and economic issues limit the translational potential of this cell processing approach. *Ex vivo* manipulation, including extraction and isolation of hMSCs, plating onto culture supports, extended culturing conditions, and harvesting the licensed hMSCs, requires an efficient manufacturing process that complies with GMP and regulatory standards [27, 28]. Furthermore, the increased cost necessary with manual or even automated processing presents a major burden that has contributed to the insolvency of many companies offering

cell therapies [29]. Therefore, generating a solution that bypasses the need for such processing would enhance the translatability and efficacy of this stem cell therapy.

Engineered biomaterials offer a potential solution for the need of *ex vivo* manipulation through scaffolds that provide necessary cues to encapsulated cells. Whereas biomaterials have been engineered to deliver factors that promote tissue healing and vascularization [30–33], relatively little research has been done in engineering a scaffold to license and enhance the immunomodulatory activities of encapsulated hMSCs. In this study, we engineered a fully synthetic and injectable scaffold to present a covalently-bound form of IFN-γ for providing a persistent licensing cue for activation of hMSCs. We demonstrate that hMSCs encapsulated within this scaffold elicit enhanced immunomodulatory properties and repair of colonic wounds in both immunocompromised and immunocompetent mouse models. This study establishes a simple, translatable, biomaterials-based strategy to enhance the immunomodulatory activities of hMSCs.

Materials and Methods

Cell culture

All human cell isolation and culture procedures were performed following IRB-approved protocols. Human mesenchymal stem cells were acquired from the NIH Resource Center at Texas A&M University and confirmed as hMSCs [34]. Briefly, cells were obtained from healthy donors via bone marrow aspirate, followed by density centrifugation for mononuclear cells and selected for adherent culture. Cells were screened for colony forming units, cell growth, and differentiation into fat and bone using standard assays. Flow cytometry analyses confirmed that cells were positive for CD90, CD105, CD73a and negative for CD34, CD11b, CD45, CD19. Received frozen stocks were thawed and grown in α-MEM containing 16% fetal bovine serum (FBS), 2 mM L-glutamine and 100 U/mL penicillin/streptomycin (ThermoFisher, MA). Human CD4+ T-cells were purified from frozen leukapheresis samples from Emory University through negative selection with a CD4 T-cell isolation kit according to the manufacturer's instructions (Biolegend, CA). Human monocytes were purified from peripheral blood mononuclear cells (PBMCs). Briefly, peripheral blood was diluted 1:1 with PBS containing 2% FBS after which the peripheral blood mononuclear cells (PBMCs) were separated via density gradient centrifugation (specific gravity: 1.077 g/mL, Stemcell Technologies, Canada). The isolated PBMCs were washed and subjected to monocyte purification using the EasySep human monocyte isolation kit (Stemcell Technologies, Canada) according to the manufacturer's instructions. All cell culture was conducted at 37 °C in a 5% CO_2 atmosphere.

PEG hydrogel synthesis and IFN-γ functionalization

Recombinant IFN-γ engineered to express a surface-exposed cysteine at amino acid position 103 (cys-IFN- γ), provided by Bolder Biotechnology, was expressed in *E. coli* and purified by ion exchanged chromatography using a S-Sepharose column as previously described [35]. Four-arm maleimide-end functionalized PEG macromer (PEG-4MAL 20kDa MW, Laysan Bio, AL, >95% purity, >95% end-functionalization) was functionalized with cys-IFN-γ for 1 hr at room temperature in phosphate buffered saline at pH=7.4. The macromer

was further functionalized with RGD peptide (GRGDSPC, final concentration 1.0 mM) (Genscript, NJ). The functionalized macromers were crosslinked using a mixture of the bi-cysteine peptide VPM (GCRDVPMSMRGGDRCG) (Genscript, NJ) and dithiothreitol (Sigma-Aldrich, MO). The concentration of cross-linker used for the synthesis of each hydrogel was calculated by matching the number of cysteines in the crosslinking solution to the number of residual maleimides following complete macromer functionalization. In certain experiments, cys-IFN-γ was substituted with the non-cysteine-containing, wild-type human recombinant IFN-γ (Biolegend, CA). Cys-IFN-γ functionalized into the PEG-4MAL hydrogel is termed 'cys-IFN-γ hydrogels' whereas non-cysteine-expressing IFN-γ mixed into the PEG-4MAL hydrogel precursor is termed 'IFN-γ hydrogels'. In experiments where cells were encapsulated in hydrogels, a pre-determined number of cells were mixed with the functionalized macromer followed by crosslinking. Hydrogels were allowed to gel at 37 °C for 10 minutes before swelling in either PBS or complete cell culture media if cells were encapsulated in the hydrogel. Tethering of cys-IFN-γ onto PEG-4MAL was determined through protein gel electrophoresis on an SDS-PAGE gel followed by protein visualization with Sypro Ruby according to manufacturer's instructions (ThermoFisher, MA). For Western blotting, cys-IFN-γ or native IFN-γ was reacted with PEG-4MAL at room temperature for 30 min. Samples were mixed in SDS-PAGE reducing sample loading buffer and denatured at 100°C for 5 min. 100 ng of Cys-IFN-γ, Cys-IFN-γ + PEG-4MAL, native IFN-γ, and native IFN-γ + PEG-4MAL were loaded per lane of BoltTM 4–12% Bis-Tris Plus Gels, separated by electrophoresis, and transferred onto a nitrocellulose membrane. Blotted membrane was blocked at room temperature for 1 hr using Odyssey Blocking Buffer in TBS (Li-Cor). Primary anti-IFN-γ (1:1,000 in blocking buffer, ab25101, Abcam) was incubated on an orbital shaker at 4°C overnight. Secondary anti-rabbit (1:10,000 in blocking buffer, IRDye 680RD goat anti-rabbit IgG, Li-Cor) was incubated on an orbital shaker at room temperature for 1 hr. Fluorescent bands were detected using the Odyssey CLx imaging system (Li-Cor).

IFN-γ release kinetics

To assess IFN-γ release kinetics from hydrogels, hydrogels were synthesized with either cys-IFN-γ or IFN-γ. Hydrogels were incubated in PBS for 4 days with supernatant collected at specified time points, snap-frozen and stored at −80°C. At day 4, the PBS from all wells was removed and replaced with fresh PBS with a subset of wells having hydrogels having cys-IFN-γ, receiving PBS with 50 μg/mL collagenase (Worthington Biochemical, NJ). Supernatants were collected at specified time points for an additional 3 days, snap-frozen and stored at −80°C. At the end of the experiment, samples were thawed and the concentration of IFN-γ assessed via ELISA (Biolegend, CA).

Bioactivity of cys-IFN-γ

hMSCs were plated onto 24-well tissue culture plastic plates at a density of 10,000 cells/cm^2. Four hr after seeding, various forms of IFN-γ were added to the cultures at a concentration of 50 ng/mL [36]. After 4 days in culture, the conditioned media was collected and frozen at −80°C. hMSCs were trypsinized, fixed, permeabilized and subjected to flow cytometric analysis on a BD Accuri C6 flow cytometer for expression of IDO and PD-L1.

Conditioned media was analyzed for secreted proteins using a custom Luminex kit (R&D Systems, MN).

Cys-IFN-γ in hydrogel-encapsulated hMSC culture

hMSCs were encapsulated in hydrogels containing cys-IFN-γ, IFN-γ or no IFN-γ as described above at a concentration of 5×10^6 cells/mL. After 4 days in culture, conditioned media was collected and frozen at −80°C. Hydrogels were then degraded by incubation in 1 mg/mL collagenase in PBS for 30 min at 37 °C. Cells were collected and subjected to flow cytometric analysis for expression of IDO and PD-L1. Conditioned media was analyzed for various proteins using a custom Luminex kit (R&D Systems, MN).

IDO activity assay

Tryptophan is converted to kynurenine through IDO activity [37]. Kynurenine was quantified using a protocol previously described [38]. Briefly, 150 μL of conditioned media after 4 days of culture in specified conditions was collected and mixed with 50 μL of 30% trichloroacetic acid. This solution was then heated to 50 °C for 10 min. Solutions were then vortexed and centrifuged at 10,000g for 5 min. 75 μL of supernatant samples were mixed with75 μL of Ehrlich's reagent and incubated for 10 min. Absorbance was then read at 492 nm.

T-cell proliferation assay

hMSCs (1×10^6 cells/mL) were encapsulated in hydrogels (20 μL) with cys-IFN-γ, IFN-γ, or no IFN-γ. For the pre-licensed group, hMSCs on tissue culture plastic were stimulated with IFN-γ for 48 hr prior to encapsulation in no IFN-γ hydrogels. To simulate *in vivo* applications in which a sink environment is present, cys-IFN-γ and IFN-γ hydrogels were washed two times over the course the first 24 hr following hydrogel synthesis. Following 48 hr of hMSC-hydrogel culture, CD4+ T-cells purified from PBMCs were resuspended in RPMI 1640 supplemented with 10% FBS, 2 mM L-glutamine, 10 mM cell-culture grade HEPES and 100 U/mL penicillin/streptomycin. CD4+ T-cells (100,000) were added to each well in a 96 well plate and stimulated with 2 μL of Dynabeads (ThermoFisher, MA). hMSC-encapsulated hydrogels were then transferred to wells containing the CD4+ T-cells and co-cultured for an additional 4 days. Eight hr prior to the end of culture, EdU was added to the media. At the end of 4 days, hydrogels were removed from the co-culture, T-cells were collected, fixed and permeabilized. T-cells were stained for DAPI and EdU that was incorporated into the T-cells upon proliferation was stained by using a Click-iT EdU kit (ThermoFisher, MA) according to manufacturer's instructions. Stained T-cells were imaged using a Nikon C2 confocal microscope and the proliferation of T-cells as quantified by taking the ratio of EdU+/total cells was performed using a custom ImageJ macro. In certain experiments, 1-methyl-L-tryptophan (1-MT) (Sigma-Aldrich, MO) was used to inhibit IDO activity. In these experiments, 1-MT was added to the media at the start of co-culture at a concentration of 1.0 mM 1-MT. T-cells were subjected to the same EdU staining protocol as described above.

Monocyte-derived dendritic cell differentiation assay

hMSCs were encapsulated in cys-IFN-γ, IFN-γ or no IFN-γ hydrogels (20 μL) at a concentration of 2.5×10^6 cells/mL. For the pre-licensed group, hMSCs on TCP were stimulated with IFN-γ for 48 hr prior to encapsulation in no IFN-γ hydrogels. To simulate *in vivo* applications in which a sink environment is present, cys-IFN-γ and IFN-γ hydrogels were washed two times over the course the first 24 hr following hydrogel synthesis. Hydrogels were cultured in this manner for 48 hr. Following 48 hr of hMSC-encapsulated hydrogel culture, purified human monocytes isolated from peripheral blood and monocytes (500,000) were added into wells of a 24-well plate. Monocytes were cultured in RPMI 1640 supplemented with 10% FBS, 2 mM L-glutamine, 100 U/mL penicillin/streptomycin, 50 ng/mL GM-CSF (Biolegend, CA) and 20 ng/mL IL-4 (Biolgend, CA). hMSC-encapsulated hydrogels were then transferred to wells containing monocytes and co-cultured for 5 days with media changes every 2–3 days. At day 5, 100 ng/mL lipopolysaccharide (LPS) (Sigma-Aldrich, MO) was added to each well to induce maturation of dendritic cells. Cells were cultured for an additional 48 hr after which the monocytes were gathered and subjected to flow cytometric analysis for CD1a, CD14, CD80 and CD86 on a BD Accuri C6 flow cytometer. In certain experiments, 1-methyl-L-tryptophan (1-MT) (Sigma-Aldrich, MO) was utilized to inhibit IDO activity. In these experiments, 1-MT was added to the media at the start of co-culture at a concentration of 1.0 mM 1-MT. The differentiated monocytes were subjected to the same flow cytometric analysis as described above.

Colonic wound surgery and injections

All animal experiments were performed with the approval of the University of Michigan Animal Care and Use Committee within the guidelines of the Guide for the Care and Use of Laboratory Animals and in accordance with the US Department of Agriculture (USDA) Animal and Plant Health Inspection Service (APHIS) regulations and the National Institutes of Health (NIH) Office of Laboratory Animal Welfare (OLAW) regulations governing the use of vertebrate animals. Colonic wounds were induced in a method similar to previously published protocols [39]. Briefly, male (8 weeks old) NOD-SCID IL2Rg-null (NSG) or C57/B6 mice (Jackson Laboratory) were anaesthetized by intraperitoneal injection of a ketamine (100 mg/kg)/xylazine (10 mg/kg) solution. A high-resolution miniaturized colonoscope system equipped with biopsy forceps (Coloview Veterinary Endoscope, Karl Stortz) was used to biopsy-injure the colonic mucosa at 5 sites along the dorsal artery. Wound size averaged approximately 1 mm^2. 50 μL hydrogel injections were performed 1 day following wounding with the aid of a custom-made device comprising a 29-gauge needle connected to a small tube. Endoscopic procedures were viewed with high-resolution (1,024 × 768 pixels) live video on a flat-panel color monitor. Each wound region was digitally photographed at day 1 and day 5 and resulting wound images for which the wound area was calculated by a blinded observer using ImageJ. Results for one mouse were averaged through quantification of the five colonic wounds/injections per mouse. To identify transplanted hMSC, tissue sections were immunostained with an antibody specific to human nuclear antigen (MAB1281, EMD Millipore).

Statistics

All experiments were performed on biological replicates. Sample size for each experimental group is reported in the appropriate figure legend. Unless otherwise noted, error bars on graphs represent SEM. Comparisons among multiple groups was performed by one-way analysis of variance (ANOVA) with post-hoc Tukey tests if data did not have significant differences in standard deviation. Data with significant differences in standard deviation were subject to log transformation after which post-hoc Tukey test performed. All statistics were performed in GraphPad Prism. A p-value of <0.05 was considered significant.

Results

Synthetic hydrogels with controlled presentation of tethered IFN-γ

We engineered hydrogels based on a maleimide-functionalized 4-armed poly(ethylene glycol)-based PEG macromer (PEG-4MAL) which allows for facile covalent tethering of peptides with a surface-accessible cysteine (Fig. 1A). In this system, IFN-γ is covalently tethered onto the macromer which is then incorporated into the hydrogel network. An adhesive peptide (RGD) was incorporated in the hydrogel to support cell activities and tissue integration. Cell-laden hydrogels were synthesized by mixing RGD peptide and hMSCs with PEG-4MAL followed by further reaction with a protease-degradable bicysteine peptide, which results in an insoluble and crosslinked PEG-based hydrogel sensitive to proteolytic degradation. Native human IFN-γ has no cysteines and thus no ability to conjugate onto the PEG-4MAL macromer without the addition of other linking reagents. To circumvent this, we utilized an IFN-γ variant that is genetically engineered to express a surface-available cysteine residue at amino acid position 103 [35]. To verify that this variant could be functionalized onto the PEG-4MAL macromer, protein gel electrophoresis was performed (Fig. 1B). Cysteine-presenting IFN-γ (cys-IFN-γ) that was not reacted with PEG-4MAL and instead mixed with PBS exhibited a distinct single band at approximately 17 kDa as expected (lane 3, ladder on lane 1). When cys-IFN-γ was reacted with PEG-4MAL macromer (20 kDa), a new band appears around 30 kDa, indicating successful conjugation (lane 2). We also performed Western blot analysis to further verify the tethered nature of the cys-IFN-γ and found a similar band around 37 kDa for the cys-IFN-γ reacted with PEG-4MAL compared to the expected single band at 17 kDa for the cys-IFN-γ reacted with PBS (Fig. S1). As expected, native IFN-γ reacted with PEG-4MAL did not show a shift in molecular weight indicative of PEGylation (Fig. S1). To further confirm the tethered nature of cys-IFN-γ on the PEG-4MAL macromer, we performed a release assay in which either cys-IFN-γ or IFN-γ was reacted with PEG-4MAL macromer and crosslinked into hydrogels using the protease-degradable peptide. We then placed the hydrogels in buffer and examined release of IFN-γ into the medium by ELISA (Fig. 1C). Hydrogels containing native IFN-γ exhibited >60% IFN-γ burst release after only 2 hr followed by complete release by 18 hr. In contrast, hydrogels containing cys-IFN-γ released ~20% of the total incorporated IFN-γ after 2 hr and after 4 days still retained approximately 65% of total incorporated protein. We attribute this initial release of cys-IFN-γ to protein that was not tethered to the hydrogel backbone. This is not unexpected as we have previously shown that a fraction (~20–30%) of other proteins (e.g., VEGF) encapsulated within PEG-4MAL gels is not covalently tethered to the hydrogel and passively released in PBS [40]. To show that the protein retained in

hydrogel is related to cys-IFN-γ tethering onto the hydrogel backbone, a subset of cys-IFN-γ-containing hydrogels were incubated for 4 days in 50 μg/mL collagenase in PBS. Addition of collagenase caused degradation of the hydrogel over the course of the following three days and resulted in complete cys-IFN-γ release. Together, the protein electrophoresis and release results confirm that the cys-IFN-γ is chemically conjugated to the PEG-4MAL macromer and subsequently tethered into the crosslinked hydrogel.

To assess whether its biological activity is affected by the chemical conjugation of the cys-IFN-γ onto PEG-4MAL macromer, hMSCs were plated on tissue-culture plastic wells and incubated in cell culture media supplemented with either cys-IFN-γ reacted with PEG-4MAL (cys-IFN-γ + PEG-4MAL), cys-IFN-γ, native IFN-γ, PEG-4MAL without IFN-γ or no treatment control for 4 days (Fig. S2, Fig. 2A). We then performed flow cytometric analysis for IDO and PD-L1 expression and assessed cytokine secretion using a Luminex kit. hMSCs incubated with cys-IFN-γ + PEG-4MAL, cys-IFN-γ, or native IFN-γ showed significantly increased levels of IDO and PD-L1 expression as assessed by median fluorescence intensity (MFI) compared to hMSCs incubated with PEG-4MAL or cell culture media alone (Fig. 2B,C). Importantly, there were no differences in IDO or PD-L1 expression among hMSCs exposed to cys-IFN-γ + PEG-4MAL, cys-IFN-γ or native IFN-γ, demonstrating that cys-IFN-γ has equivalent biological activity to the native protein and that conjugation to PEG-4MAL macromer does not affect its activity. Moreover, the concentrations of secreted IL-6, CXCL10, CCL2, CCL8, and M-CSF were all significantly increased while VEGF was significantly decreased in hMSCs exposed to cys-IFN-γ + PEG-4MAL, the cys-IFN-γ or native IFN-γ compared to groups not treated with IFN-γ (Fig. 2D–I). No significant differences were noted among cys-IFN-γ + PEG-4MAL, cys-IFN-γ and native IFN-γ for IL-6. However, cys-IFN-γ + PEG-4MAL did show decreases in CXCL10, CCL2, CCL8 and M-CSF concentrations compared to cys-IFN-γ without PEG-4MAL and native IFN-γ, reflecting a slight loss in activity resulting from PEGylation. Nevertheless, the cys-IFN-γ + PEG-4MAL exhibits significantly higher activity than the negative controls.

Enhanced hMSC immunoactivation in hydrogels with tethered IFN-γ

We next examined whether hydrogels presenting cys-IFN-γ modulate the immunomodulatory phenotype of encapsulated-hMSCs (Fig. 3A). hMSCs were encapsulated in hydrogels engineered with different doses of cys-IFN-γ ranging from 0–500 ng in a 20 μL hydrogel (final concentration 0–25 μg/mL) to assess the dose response of hMSCs to cys-IFN-γ. No differences in cell viability or growth were observed after encapsulation among hydrogel groups. Following 4 days in culture, hMSCs were subjected to flow cytometric analysis for PDL1 (Fig. S3) and IDO (Fig. 3B). Expression of PD-L1 decreased as the concentration of cys-IFN-γ increased from 0 to 80 ng but then increased from 80 to 500 ng. While PD-L1 expression increased at doses of 80 ng of cys-IFN-γ and higher, PD-L1 expression was not significantly different at 500 ng, the highest dose tested, compared to basal expression levels. Notably, IDO expression increased with cys-IFN-γ concentration in a dose-dependent fashion with doses greater than 10 ng showing a significant increase in IDO compared to basal IDO levels (Fig. 3B). We also confirmed that increased IDO expression correlated with increased IDO activity by measuring the

concentration of kynurenine, the product of tryptophan after its catalysis by IDO (Fig. S4). For subsequent studies, we used a concentration of 25 μg/mL of IFN-γ within the hydrogel because this dose yielded the highest IDO expression in encapsulated hMSC.

We next sought to understand how the polymer density of the hydrogel, which controls the mechanical properties and diffusivity of the gel, influences the expression of IDO and PD-L1 for encapsulated hMSCs as polymer density may affect the availability of biological agents to encapsulated cells [41]. hMSC-laden hydrogels of differing polymer densities ranging from 4% to 10% were synthesized with a constant 25 μg/mL concentration of cys-IFN-γ. Following 4 days in culture, hMSCs were subjected to flow cytometric analysis for expression of IDO and PD-L1 (Fig. S5). Whereas no differences were noted for PD-L1 expression as a function of polymer density, hMSCs within 10% hydrogels exhibited significantly lower levels of expression of IDO compared to those in 4%, 6% and 8% hydrogels. Together, these results show that the expression of IDO is significantly influenced by the dose of cys-IFN-γ and the polymer density of the surrounding biomaterial environment. Based on these results, we chose to focus on 6% hydrogels with 25 μg/mL IFN-γ for subsequent *in vitro* experiments as these conditions correlated with the highest level of hMSC-based IDO expression.

cys-IFN-γ hydrogels enhance hMSC immunomodulatory activities

A potential advantage of presenting IFN-γ tethered to the hydrogel microenvironment is enhanced and sustained licensing compared to stimulation with soluble IFN-γ. We therefore examined whether IFN-γ tethering to the hydrogel increases licensing duration compared to soluble IFN-γ. hMSCs were encapsulated in hydrogels with either cys-IFN-γ, IFN-γ or no IFN-γ. Following encapsulation, hydrogels were washed throughout the first 24 hr to simulate sink conditions present *in vivo*. Hydrogels were then cultured for an additional 3 days after which the hydrogels were degraded, conditioned media collected for cytokine analysis, and hMSCs stained for IDO and PD-L1 followed by flow cytometric analysis (Fig. 3C,D). hMSCs encapsulated in hydrogels containing soluble IFN-γ exhibited increased IDO and PD-L1 expression compared to control hMSCs. Importantly, hMSCs encapsulated in hydrogels with tethered cys-IFN-γ showed significantly increased IDO and PD-L1 expression compared to hMSCs encapsulated in hydrogels containing soluble IFN-γ as well as control unstimulated hMSCs. Furthermore, analysis of conditioned media showed that hMSCs encapsulated in cys-IFN-γ-tethered hydrogels secreted increased levels of MCP-1, M-CSF, CXCL9, CXCL10 and CCL8 compared to hMSCs encapsulated in either IFN-γ-containing hydrogels or cells encapsulated in control hydrogels without IFN-γ (Fig. 3E–I). In addition, hMSCs encapsulated in cys-IFN-γ-tethered hydrogels had equivalent levels of IL-6, CXCL8, and VEGF as cells encapsulated in IFN-γ-containing hydrogels, and these levels were suppressed compared to control hMSC not exposed to IFN-γ (Fig. S6). Collectively, these results show that cys-IFN-γ-tethered hydrogels significantly alter hMSC phenotype by augmenting the expression and release of immunomodulatory factors.

IFN-γ-stimulated hMSCs reduce the proliferation of activated T-cells when co-cultured [7]. We next assessed whether cys-IFN-γ-tethered hydrogels augment the inhibitory effect of hMSCs on T-cell proliferation (Fig 4A). hMSCs were encapsulated in hydrogels presenting

either cys-IFN-γ or IFN-γ and gels with no IFN-γ. Hydrogels were washed twice within 24 hr following encapsulation to simulate a sink effect *in vivo*. To compare with hMSCs licensed with soluble IFN-γ as routinely done in the literature, we included a group of hMSCs encapsulated in hydrogels without IFN-γ and incubated in media containing 500 ng/mL IFN-γ (pre-licensed hMSCs). hMSC-laden hydrogels were co-cultured with activated CD4+ human T-cells for 4 days after which the T-cells were stained for EdU and CD3 to examine proliferation and verify their T-cell phenotype, respectively (Fig. 4B–G). Activated T-cells cultured solely with Dynabeads (to activate T-cells) showed a similar high degree of proliferation compared to activated T-cells cultured with cys-IFN-γ-tethered hydrogel without hMSCs indicating that the presence of the cys-IFN-γ hydrogel by itself has no effect on T-cell proliferation (Fig. 4H). Furthermore, these two groups showed significantly greater levels of T-cell proliferation compared to all groups having IFN-γ. Importantly, T-cells incubated with hMSCs in cys-IFN-γ-tethered hydrogels exhibited significantly lower levels of proliferation compared to T-cells cultured with hMSCs in hydrogels containing IFN-γ, demonstrating augmented immunomodulatory properties for hMSCs encapsulated in gels with tethered IFN-γ compared to gels with soluble IFN-γ. There were no differences in T-cell proliferation for T-cells incubated with hMSCs in cys-IFN-γ-tethered hydrogels and hydrogels with pre-licensed hMSCs.

We next examined the role of IDO produced by hMSCs in this inhibitory effect. hMSCs were encapsulated in cys-IFN-γ-tethered hydrogels and co-cultured with human T-cells in the presence or absence of the IDO inhibitor, 1-methyl-tryptophan (1-MT)(Fig. 4I). After 4 days, T-cells incubated with hMSCs encapsulated in cys-IFN-γ-tethered hydrogels in the absence of 1-MT exhibited significantly reduced proliferation compared to T-cells cultured in the same conditions in the presence of 1-MT. Importantly, T-cells cultured with 1-MT either with or without hMSCs showed no difference in proliferation. Together, these results show that addition of 1-MT completely inhibited the anti-proliferative effect of licensed hMSCs in the co-culture. This complete abrogation of anti-proliferative effect indicates that IDO is a key regulator of the anti-proliferative activities of hydrogel-encapsulated hMSCs.

In addition to inhibiting T-cell proliferation, IFN-γ-licensed hMSCs inhibit the differentiation of monocytes into dendritic cells *in vitro* [6]. We thus assessed whether cys-IFN-γ-tethered hydrogels augment the inhibition of dendritic cell differentiation. Untreated or pre-licensed hMSCs were encapsulated within hydrogels containing cys-IFN-γ or IFN-γ and hydrogels containing no IFN-γ and co-cultured with peripheral blood purified CD14+ human monocytes. These cells were co-cultured in dendritic cell differentiation conditions for 5 days. Monocyte differentiation was performed by addition of 100 ng/mL LPS for an additional 2 days. Following complete differentiation, monocytes were stained for the monocyte marker CD14, the dendritic cell marker CD1a and maturation markers CD80 and CD86. Monocytes cultured in the absence of hMSCs exhibited significantly greater dendritic cell differentiation compared to monocytes co-cultured with hMSCs as quantified by the percentage of CD1a+/CD14- cells (Fig. 4J). Monocytes cultured with hydrogels encapsulating untreated hMSCs, hMSCs exposed to soluble IFN-γ (pre-licensed), or hMSCs encapsulated in hydrogels containing IFN-γ showed lower dendritic cell differentiation than monocytes differentiated in the absence of hMSCs, and there were no differences in dendritic cell differentiation among these hMSC-containing groups.

Remarkably, monocytes cultured with hMSCs encapsulated in cys-IFN-γ-tethered hydrogels showed a significant reduction in their dendritic cell differentiation compared to monocytes cultured with all other IFN-γ-treated hMSC conditions. Furthermore, monocytes cultured with hMSCs encapsulated in cys-IFN-γ-tethered hydrogels displayed lower expression of maturation markers CD80 and CD86 compared to monocytes cultured in all other conditions tested (Fig. 4K,L). These results show that hMSCs in cys-IFN-γ-tethered hydrogels exhibit significantly upregulated ability to inhibit monocyte-derived dendritic cell differentiation compared to either hMSCs not exposed to IFN-γ or hMSCs in IFN-γ hydrogels.

We next investigated the mechanism of action for this effect by co-culturing human monocytes with hMSCs encapsulated in cys-IFN-γ-tethered hydrogels in the absence or presence of either an IDO inhibitor (1-MT), a PGE2 inhibitor (NS-398), or both. Following 7 days in dendritic cell differentiation conditions, monocytes were collected, stained for CD1a and CD14 and subjected to flow cytometric analysis (Fig. S7). Without the addition of IDO or PGE2 inhibitor, monocytes co-cultured with hMSCs in cys-IFN-γ-tethered hydrogels showed lower dendritic cell differentiation compared to monocytes that were not co-cultured with hMSCs. Monocytes co-cultured with encapsulated hMSC and exposed to the IDO or PGE2 inhibitor exhibited higher dendritic cell differentiation compared to vehicle only controls. The IDO inhibitor had a more pronounced effect than the PGE2 inhibitor, demonstrating that IDO is the dominant mechanism inhibiting dendritic cell differentiation for hMSCs encapsulated in cys-IFN-γ-tethered hydrogels.

hMSCs in cys-IFN-γ-tethered hydrogels accelerate healing of mucosal wounds

The use of hMSCs for treating inflammatory diseases in clinical trials has rapidly grown in recent years with Crohn's and other inflammatory bowel diseases consisting a large portion of the conditions being treated [42]. In addition, previous literature suggests that licensing hMSCs with IFN-γ can significantly augment the regenerative effects of cell therapy in pre-clinical colitis models [43]. We thus tested whether hMSCs encapsulated within cys-IFN-γ-tethered hydrogels enhance repair of intestinal mucosal wounds. A major advantage of the hydrogel platform is the ability to formulate the scaffold as an injectable delivery vehicle. Because the degradation profile of the hydrogel is an important parameter influencing healing responses, we used hydrogels crosslinked with a protease-degradable crosslinking peptide (VPM) that previously supported *in vivo* delivery of therapeutic proteins and excellent tissue healing [44–47]. We first investigated the effects on wound regeneration of hMSCs delivered within cys-IFN-γ-tethered hydrogels compared to either untreated control wounds, wounds injected with hMSCs in saline, and wounds treated with control hydrogels containing hMSCs. Wounds were mechanically induced within the colon of immunocompromised NSG mice using a veterinary colonoscope as described previously [39]. Twenty-four hr following injury, the prescribed treatments were injected at the site of injury and videos of the wounds taken. Five days following treatment, progression of wound repair was recorded and healing was assessed by comparing the wound area on day 5 to the wound area on day 1. Remarkably, wounds treated with hMSCs delivered within cys-IFN-γ-tethered hydrogels enhanced wound healing compared to control untreated wounds (Fig. S8). Importantly, no other groups tested displayed differences compared to the control untreated wounds.

We conducted a follow-up experiment where colonic mucosal wounds in immunocompetent C57/B6 mice were treated with hMSCs delivered within cys-IFN-γ-tethered hydrogels or cys-IFN-γ-tethered hydrogels without hMSCs. The use of C57/B6 mice ensures an active immune system that is more physiologically relevant to clinical cases. Other groups tested included colonic wounds injected with hMSCs in saline and wounds injected with un-crosslinked hydrogel components. Five days post-injury, wound closure was assessed as previously described. No differences in wound closure were noted between mice receiving un-crosslinked hydrogel components and mice injected with either hMSCs in saline or hydrogel-encapsulated hMSCs without cys-IFN-γ. In contrast, hMSCs delivered within cys-IFN-γ-tethered hydrogels exhibited significantly increased wound closure at day 5 post-injury compared to control mice receiving un-crosslinked hydrogel components and mice receiving cys-IFN-γ gels without hMSCs (Fig. 5A). Histological sections confirm this finding showing that mice treated with cys-IFN-γ-tethered hydrogels with hMSCs had smaller wounds compared to the other groups tested (Fig. 5B–E). Notably, wounds treated with cys-IFN-γ-tethered hydrogels with hMSCs showed the presence of crypts re-forming within the repair tissue, indicating healing at a more advanced stage compared other groups. Additionally, wounds examined at 4 weeks post-injection showed the presence of implanted hMSCs, demonstrating persistence of cells that correlates with enhanced wound closure (Fig. S9).

Discussion

With the impetus for cell therapies to be translated into the clinic, hMSCs have been evaluated in nearly 500 clinical trials [48]. While these cells were initially pursued for their differentiation potential, recent evidence, including their effects in treating inflammatory diseases such as GvHD and Crohn's disease, support their use for their immunomodulatory properties [49, 50]. Nonetheless, the success of these clinical trials in treating inflammatory diseases has been mixed with approximately half of patients treated with hMSCs showing little to no improvement [14–17]. Therefore, there is significant need for increasing the efficacy of these stem cell-based therapies and specifically, increasing the immunomodulatory properties of hMSCs. Licensing hMSCs with IFN-γ increases their immunomodulatory properties in *in vitro* and *in vivo* systems [51]. However, the need for *ex vivo* manipulation of hMSCs with IFN-γ raises considerable barriers including increased costs, clearing regulatory hurdles, and establishing rigorous and reliable cell handling practices that impact clinical translation [27]. Engineering a biomaterial that can license hMSCs without the need for *ex vivo* manipulation can significantly enhance the translation of hMSC-based stem cell therapies.

Previous research has described the conjugation of bioactive proteins to biomaterials scaffolds to boost stem cell activities [52–55]. In this study, we engineered a novel strategy for licensing hMSCs by functionalizing a PEG-based hydrogel with a biologically active form of IFN-γ. To assess the functionality and efficacy of our platform, we tested two general concepts: 1) whether the scaffold modification elicited a response in scaffold-encapsulated hMSCs, and 2) whether the effect imparted onto the hMSCs generated secondary effects on immune cells. hMSCs encapsulated within IFN-γ-presenting hydrogels exhibited similar or increased expression of both cell-licensing markers IDO and PD-L1

compared to hMSCs that were pre-licensed with soluble IFN-γ. Furthermore, hMSCs encapsulated within IFN-γ-presenting hydrogels showed a potent ability to inhibit both activated human T-cell proliferation and monocyte-derived dendritic cell differentiation. Importantly, the inhibition of dendritic cell differentiation imparted by hMSCs encapsulated within IFN-γ-tethered hydrogels was greater than that of encapsulated hMSCs that were licensed with soluble IFN-γ prior to co-culture. This increased effect for the tethered IFN-γ is likely due to the increased duration of licensing as the tethered form is present throughout the co-culture period while the unbound IFN-γ will be washed away. In addition to the increased duration, the tethered form of IFN-γ may also result in higher local concentrations of IFN-γ surrounding the encapsulated hMSCs compared to the unbound form. Future studies will examine whether lower doses of cys-IFN-γ could be utilized thus furthering the applicability of clinical use.

Within a functional model, hMSCs encapsulated in IFN-γ-presenting hydrogels exhibited significantly higher levels of mucosal wound closure compared to untreated controls as well as wounds treated with hMSCs in hydrogels. This finding supports the notion that the effects imparted by licensing hMSCs elicits a functional response *in vivo*. Further studies are necessary to elucidate how such licensing influences the cellular and molecular cascades within the affected area in order to further increase the efficacy of the therapy.

Supplementary Material

Refer to Web version on PubMed Central for supplementary material.

Acknowledgements:

We thank Lana Anderson for technical assistance in preparing the cys-IFN-γ protein.

Funding: Research reported in this publication was supported by the National Institute of Arthritis and Musculoskeletal and Skin Diseases of the National Institutes of Health under Award Number R01AR062368 (A.J.G.) and R01DK055679 (A.N.) and the National Science Foundation Engineering Research Center for Cell Manufacturing Technologies (CMaT) under Award Number 1648035. M.Q. is funded by a Crohn's and Colitis Foundation Career Development Award (544599). The content is solely the responsibility of the authors and does not necessarily represent the official views of the National Institutes of Health.

REFERENCES

[1]. Bruder SP, Fink DJ, Caplan AI. Mesenchymal stem cells in bone development, bone repair, and skeletal regeneration therapy. J Cell Biochem. 1994;56:283–94. [PubMed: 7876320]

[2]. Caplan AI. Adult mesenchymal stem cells for tissue engineering versus regenerative medicine. J Cell Physiol. 2007;213:341–7. [PubMed: 17620285]

[3]. Aggarwal S, Pittenger MF. Human mesenchymal stem cells modulate allogeneic immune cell responses. Blood. 2005;105:1815–22. [PubMed: 15494428]

[4]. Wang Y, Chen X, Cao W, Shi Y. Plasticity of mesenchymal stem cells in immunomodulation: pathological and therapeutic implications. Nat Immunol. 2014;15:1009–16. [PubMed: 25329189]

[5]. Gao F, Chiu SM, Motan DA, Zhang Z, Chen L, Ji HL, et al. Mesenchymal stem cells and immunomodulation: current status and future prospects. Cell Death Dis. 2016;7:e2062. [PubMed: 26794657]

[6]. Spaggiari GM, Abdelrazik H, Becchetti F, Moretta L. MSCs inhibit monocyte-derived DC maturation and function by selectively interfering with the generation of immature DCs: central role of MSC-derived prostaglandin E2. Blood. 2009;113:6576–83. [PubMed: 19398717]

[7]. Meisel R, Zibert A, Laryea M, Gobel U, Daubener W, Dilloo D. Human bone marrow stromal cells inhibit allogeneic T-cell responses by indoleamine 2,3-dioxygenase-mediated tryptophan degradation. Blood. 2004;103:4619–21. [PubMed: 15001472]

[8]. Spaggiari GM, Capobianco A, Abdelrazik H, Becchetti F, Mingari MC, Moretta L. Mesenchymal stem cells inhibit natural killer-cell proliferation, cytotoxicity, and cytokine production: role of indoleamine 2,3-dioxygenase and prostaglandin E2. Blood. 2008;111:1327–33. [PubMed: 17951526]

[9]. Corcione A, Benvenuto F, Ferretti E, Giunti D, Cappiello V, Cazzanti F, et al. Human mesenchymal stem cells modulate B-cell functions. Blood. 2006;107:367–72. [PubMed: 16141348]

[10]. Auletta JJ, Eid SK, Wuttisarnwattana P, Silva I, Metheny L, Keller MD, et al. Human mesenchymal stromal cells attenuate graft-versus-host disease and maintain graft-versus-leukemia activity following experimental allogeneic bone marrow transplantation. Stem Cells. 2015;33:601–14. [PubMed: 25336340]

[11]. Wang X, Kimbrel EA, Ijichi K, Paul D, Lazorchak AS, Chu J, et al. Human ESC-derived MSCs outperform bone marrow MSCs in the treatment of an EAE model of multiple sclerosis. Stem Cell Reports. 2014;3:115–30. [PubMed: 25068126]

[12]. Gonzalez MA, Gonzalez-Rey E, Rico L, Buscher D, Delgado M. Adipose-derived mesenchymal stem cells alleviate experimental colitis by inhibiting inflammatory and autoimmune responses. Gastroenterology. 2009;136:978–89. [PubMed: 19135996]

[13]. Yanez R, Lamana ML, Garcia-Castro J, Colmenero I, Ramirez M, Bueren JA. Adipose tissue-derived mesenchymal stem cells have in vivo immunosuppressive properties applicable for the control of the graft-versus-host disease. Stem Cells. 2006;24:2582–91. [PubMed: 16873762]

[14]. Forbes GM, Sturm MJ, Leong RW, Sparrow MP, Segarajasingam D, Cummins AG, et al. A phase 2 study of allogeneic mesenchymal stromal cells for luminal Crohn's disease refractory to biologic therapy. Clin Gastroenterol Hepatol. 2014;12:64–71. [PubMed: 23872668]

[15]. Le Blanc K, Frassoni F, Ball L, Locatelli F, Roelofs H, Lewis I, et al. Mesenchymal stem cells for treatment of steroid-resistant, severe, acute graft-versus-host disease: a phase II study. Lancet. 2008;371:1579–86. [PubMed: 18468541]

[16]. Resnick IB, Barkats C, Shapira MY, Stepensky P, Bloom AI, Shimoni A, et al. Treatment of severe steroid resistant acute GVHD with mesenchymal stromal cells (MSC). Am J Blood Res. 2013;3:225–38. [PubMed: 23997985]

[17]. Panes J, Garcia-Olmo D, Van Assche G, Colombel JF, Reinisch W, Baumgart DC, et al. Expanded allogeneic adipose-derived mesenchymal stem cells (Cx601) for complex perianal fistulas in Crohn's disease: a phase 3 randomised, double-blind controlled trial. Lancet. 2016;388:1281–90. [PubMed: 27477896]

[18]. Krampera M, Cosmi L, Angeli R, Pasini A, Liotta F, Andreini A, et al. Role for interferon-gamma in the immunomodulatory activity of human bone marrow mesenchymal stem cells. Stem Cells. 2006;24:386–98. [PubMed: 16123384]

[19]. Lee MW, Ryu S, Kim DS, Sung KW, Koo HH, Yoo KH. Strategies to improve the immunosuppressive properties of human mesenchymal stem cells. Stem Cell Res Ther. 2015;6:179. [PubMed: 26445096]

[20]. Polchert D, Sobinsky J, Douglas G, Kidd M, Moadsiri A, Reina E, et al. IFN-gamma activation of mesenchymal stem cells for treatment and prevention of graft versus host disease. Eur J Immunol. 2008;38:1745–55. [PubMed: 18493986]

[21]. Liang C, Jiang E, Yao J, Wang M, Chen S, Zhou Z, et al. Interferon-gamma mediates the immunosuppression of bone marrow mesenchymal stem cells on T-lymphocytes in vitro. Hematology. 2018;23:44–9. [PubMed: 28581352]

[22]. Jin P, Zhao Y, Liu H, Chen J, Ren J, Jin J, et al. Interferon-gamma and tumor necrosis factor-alpha polarize bone marrow stromal cells uniformly to a Th1 phenotype. Sci Rep 2016;6:26345. [PubMed: 27211104]

[23]. Bernardo ME, Fibbe WE. Mesenchymal stromal cells: sensors and switchers of inflammation. Cell Stem Cell. 2013;13:392–402. [PubMed: 24094322]

[24]. Shi Y, Su J, Roberts AI, Shou P, Rabson AB, Ren G. How mesenchymal stem cells interact with tissue immune responses. Trends Immunol. 2012;33:136–43. [PubMed: 22227317]

[25]. Chinnadurai R, Copland IB, Patel SR, Galipeau J. IDO-independent suppression of T cell effector function by IFN-gamma-licensed human mesenchymal stromal cells. J Immunol. 2014;192:1491–501. [PubMed: 24403533]

[26]. Duijvestein M, Wildenberg ME, Welling MM, Hennink S, Molendijk I, van Zuylen VL, et al. Pretreatment with interferon-gamma enhances the therapeutic activity of mesenchymal stromal cells in animal models of colitis. Stem Cells. 2011;29:1549–58. [PubMed: 21898680]

[27]. Heathman TR, Nienow AW, McCall MJ, Coopman K, Kara B, Hewitt CJ. The translation of cell-based therapies: clinical landscape and manufacturing challenges. Regen Med. 2015;10:49–64. [PubMed: 25562352]

[28]. Tarnowski J, Krishna D, Jespers L, Ketkar A, Haddock R, Imrie J, et al. Delivering advanced therapies: the big pharma approach. Gene Ther. 2017;24:593–8. [PubMed: 28737744]

[29]. Dodson BP, Levine AD. Challenges in the translation and commercialization of cell therapies. BMC Biotechnol. 2015;15:70. [PubMed: 26250902]

[30]. Veith AP, Henderson K, Spencer A, Sligar AD, Baker AB. Therapeutic strategies for enhancing angiogenesis in wound healing. Adv Drug Deliv Rev. 2018; S0169–409X(18)30246–1.

[31]. Chuang CK, Lin KJ, Lin CY, Chang YH, Yen TC, Hwang SM, et al. Xenotransplantation of human mesenchymal stem cells into immunocompetent rats for calvarial bone repair. Tissue Eng Part A. 2010;16:479–88. [PubMed: 19702514]

[32]. Lee K, Silva EA, Mooney DJ. Growth factor delivery-based tissue engineering: general approaches and a review of recent developments. J R Soc Interface. 2011;8:153–70. [PubMed: 20719768]

[33]. Annabi N, Tamayol A, Uquillas JA, Akbari M, Bertassoni LE, Cha C, et al. 25th anniversary article: Rational design and applications of hydrogels in regenerative medicine. Adv Mater. 2014;26:85–123. [PubMed: 24741694]

[34]. Dominici M, Le Blanc K, Mueller I, Slaper-Cortenbach I, Marini F, Krause D, et al. Minimal criteria for defining multipotent mesenchymal stromal cells. The International Society for Cellular Therapy position statement. Cytotherapy. 2006;8:315–7. [PubMed: 16923606]

[35]. Fam CM, Eisenberg SP, Carlson SJ, Chlipala EA, Cox GN, Rosendahl MS. PEGylation improves the pharmacokinetic properties and ability of interferon gamma to inhibit growth of a human tumor xenograft in athymic mice. J Interferon Cytokine Res. 2014;34:759–68. [PubMed: 24841172]

[36]. Klinker MW, Marklein RA, Lo Surdo JL, Wei CH, Bauer SR. Morphological features of IFN-gamma-stimulated mesenchymal stromal cells predict overall immunosuppressive capacity. Proc Natl Acad Sci U S A. 2017;114:E2598–e607. [PubMed: 28283659]

[37]. Grohmann U, Fallarino F, Puccetti P. Tolerance, DCs and tryptophan: much ado about IDO. Trends Immunol. 2003;24:242–8. [PubMed: 12738417]

[38]. Zhang Q, Shi S, Liu Y, Uyanne J, Shi Y, Shi S, et al. Mesenchymal stem cells derived from human gingiva are capable of immunomodulatory functions and ameliorate inflammation-related tissue destruction in experimental colitis. J Immunol. 2009;183:7787–98. [PubMed: 19923445]

[39]. Cruz-Acuna R, Quiros M, Farkas AE, Dedhia PH, Huang S, Siuda D, et al. Synthetic hydrogels for human intestinal organoid generation and colonic wound repair. Nat Cell Biol. 2017;19:1326–35. [PubMed: 29058719]

[40]. Garcia JR, Clark AY, Garcia AJ. Integrin-specific hydrogels functionalized with VEGF for vascularization and bone regeneration of critical-size bone defects. J Biomed Mater Res A. 2016;104:889–900. [PubMed: 26662727]

[41]. Stevens MM, George JH. Exploring and engineering the cell surface interface. Science. 2005;310:1135–8. [PubMed: 16293749]

[42]. Mao F, Tu Q, Wang L, Chu F, Li X, Li HS, et al. Mesenchymal stem cells and their therapeutic applications in inflammatory bowel disease. Oncotarget. 2017;8:38008–21. [PubMed: 28402942]

[43]. Chen Y, Song Y, Miao H, Xu Y, Lv M, Wang T, et al. Gene delivery with IFN-gamma-expression plasmids enhances the therapeutic effects of MSCs on DSS-induced mouse colitis. Inflamm Res. 2015;64:671–81. [PubMed: 26153869]

[44]. Phelps EA, Headen DM, Taylor WR, Thule PM, Garcia AJ. Vasculogenic bio-synthetic hydrogel for enhancement of pancreatic islet engraftment and function in type 1 diabetes. Biomaterials. 2013;34:4602–11. [PubMed: 23541111]

[45]. Shekaran A, Garcia JR, Clark AY, Kavanaugh TE, Lin AS, Guldberg RE, et al. Bone regeneration using an alpha 2 beta 1 integrin-specific hydrogel as a BMP-2 delivery vehicle. Biomaterials. 2014;35:5453–61. [PubMed: 24726536]

[46]. Weaver JD, Headen DM, Aquart J, Johnson CT, Shea LD, Shirwan H, et al. Vasculogenic hydrogel enhances islet survival, engraftment, and function in leading extrahepatic sites. Sci Adv. 2017;3:e1700184. [PubMed: 28630926]

[47]. Johnson CT, Wroe JA, Agarwal R, Martin KE, Guldberg RE, Donlan RM, et al. Hydrogel delivery of lysostaphin eliminates orthopedic implant infection by Staphylococcus aureus and supports fracture healing. Proc Natl Acad Sci U S A. 2018;115:E4960–e9. [PubMed: 29760099]

[48]. Squillaro T, Peluso G, Galderisi U. Clinical Trials With Mesenchymal Stem Cells: An Update. Cell Transplant. 2016;25:829–48. [PubMed: 26423725]

[49]. Klinker MW, Wei CH. Mesenchymal stem cells in the treatment of inflammatory and autoimmune diseases in experimental animal models. World J Stem Cells. 2015;7:556–67. [PubMed: 25914763]

[50]. Wang LT, Ting CH, Yen ML, Liu KJ, Sytwu HK, Wu KK, et al. Human mesenchymal stem cells (MSCs) for treatment towards immune- and inflammation-mediated diseases: review of current clinical trials. J Biomed Sci. 2016;23:76. [PubMed: 27809910]

[51]. Krampera M Mesenchymal stromal cell ‘licensing’: a multistep process. Leukemia. 2011;25:1408–14. [PubMed: 21617697]

[52]. Cosgrove BD, Mui KL, Driscoll TP, Caliari SR, Mehta KD, Assoian RK, et al. N-cadherin adhesive interactions modulate matrix mechanosensing and fate commitment of mesenchymal stem cells. Nat Mater. 2016;15:1297–306. [PubMed: 27525568]

[53]. Li H, Koenig AM, Sloan P, Leipzig ND. In vivo assessment of guided neural stem cell differentiation in growth factor immobilized chitosan-based hydrogel scaffolds. Biomaterials. 2014;35:9049–57. [PubMed: 25112933]

[54]. Li R, Xu J, Wong DSH, Li J, Zhao P, Bian L. Self-assembled N-cadherin mimetic peptide hydrogels promote the chondrogenesis of mesenchymal stem cells through inhibition of canonical Wnt/beta-catenin signaling. Biomaterials. 2017;145:33–43. [PubMed: 28843065]

[55]. Zhang K, Jia Z, Yang B, Feng Q, Xu X, Yuan W, et al. Adaptable hydrogels mediate cofactor-assisted activation of biomarker-responsive drug delivery via positive feedback for enhanced tissue regeneration. Adv Sci. 2018;5:1800875.

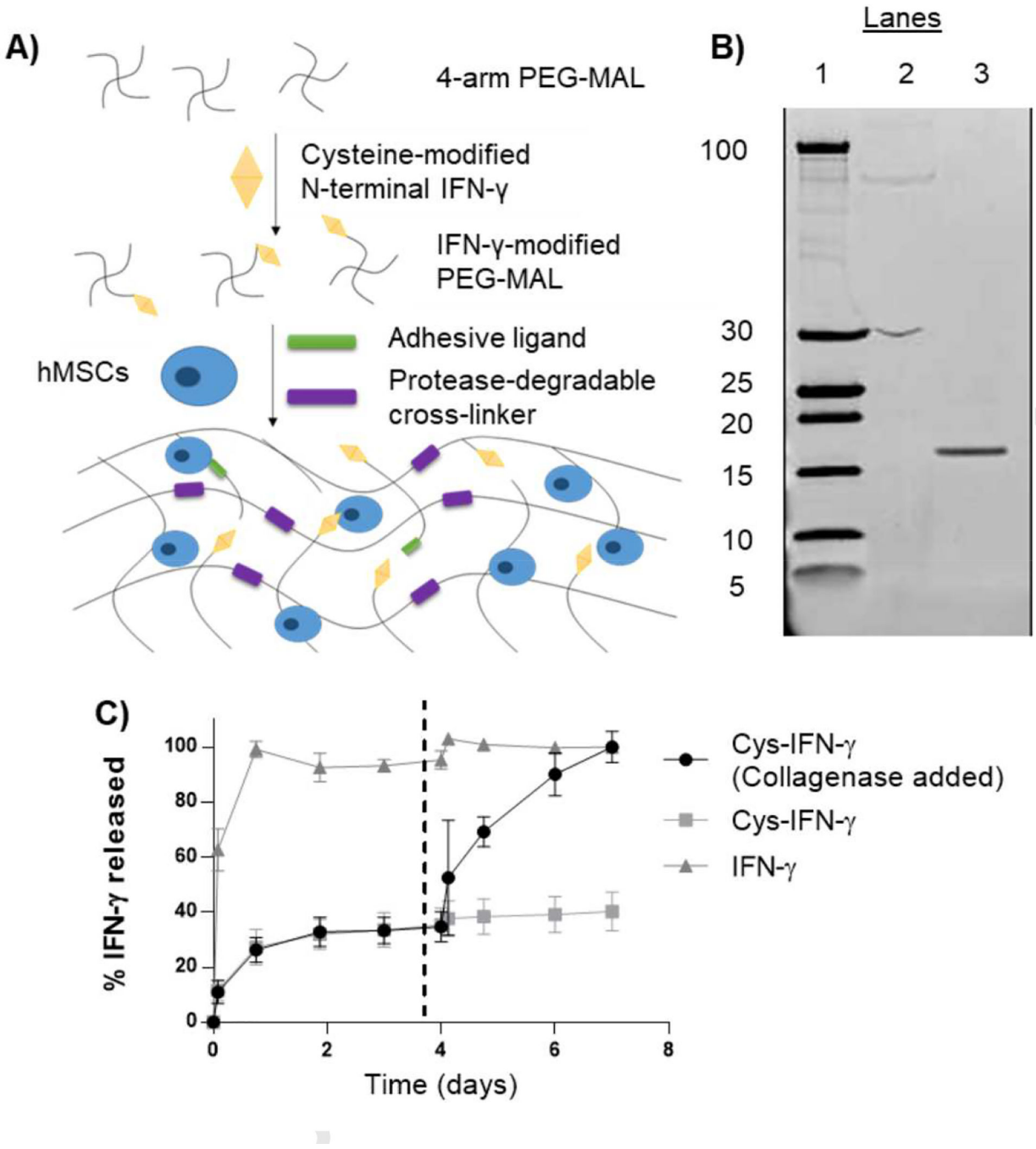

Figure 1.

Tethering of cys-IFN-γ onto PEG-4MAL hydrogels and degradation-dependent release. (A) Schematic representing cytokine functionalization with adhesive ligand, hMSC and protease-degradable cross-linker incorporation. (B) Protein gel electrophoresis for cys-IFN-γ reacted with PEG-4MAL. Lane 1) protein ladder, lane 2) cys-IFN-γ reacted with PEG-4-MAL, lane 3) cys-IFN-γ. (C) Cys-IFN-γ release kinetics as measured by ELISA. All groups were incubated in PBS until 4 days at which point collagenase (50 μg/mL) was added to the respective group. N=5. Error bars ± SEM.

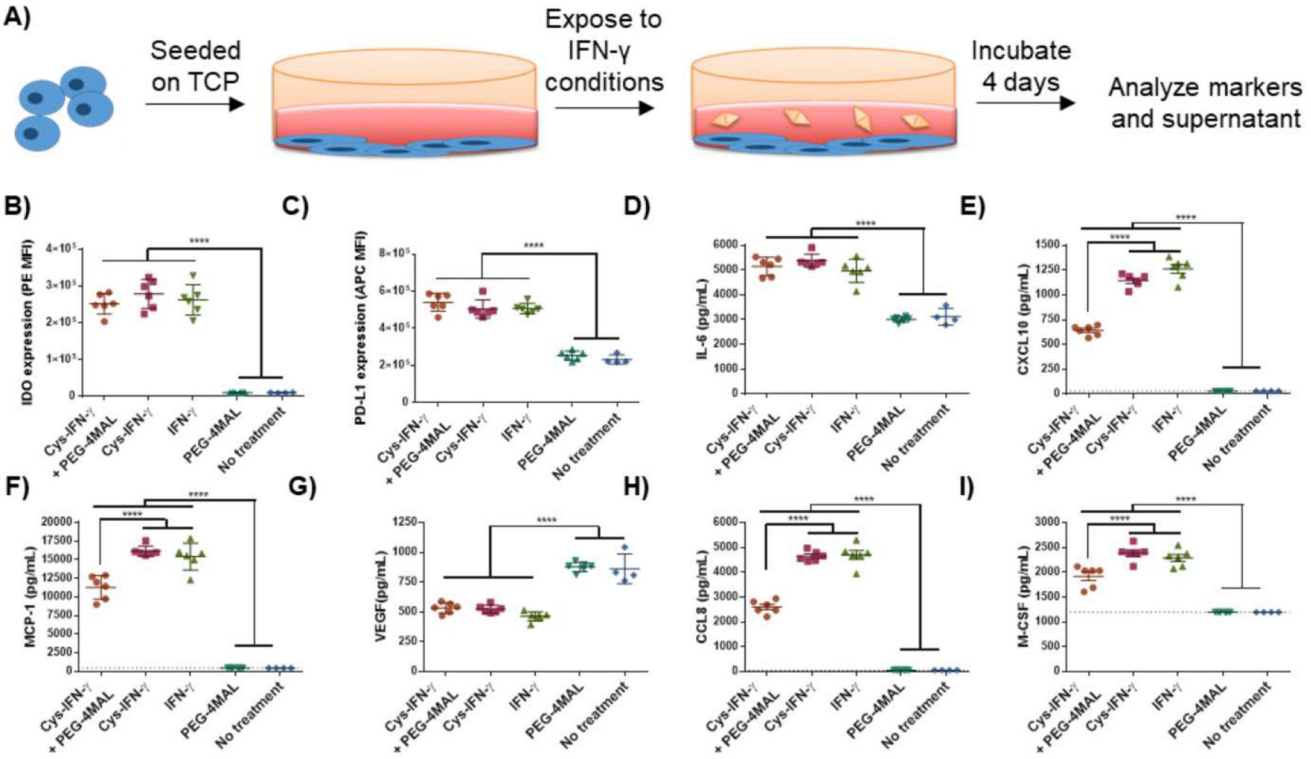

Figure 2.

hMSCs on tissue culture plastic exhibit significant changes in marker expression and secreteome when incubated with IFN-γ compared to hMSCs without IFN-γ. A) Schematic of experimental outline. hMSCs were incubated with either cys-IFN-γ + PEG-4MAL, cys-IFN-γ, native IFN-γ, PEG-4MAL or no treatment. Following 4 days, hMSCs were stained for B) IDO and C) PD-L1 and subjected to flow cytometry. Conditioned media was analyzed for concentrations of various proteins including D) IL-6, E) CXCL10, F) MCP-1, G) VEGF, H) CCL8 and I) M-CSF. Dotted lines signify limit of detection for specific protein. N=6. Error bars ± SEM. One-way ANOVA **** $p < 0.0001$.

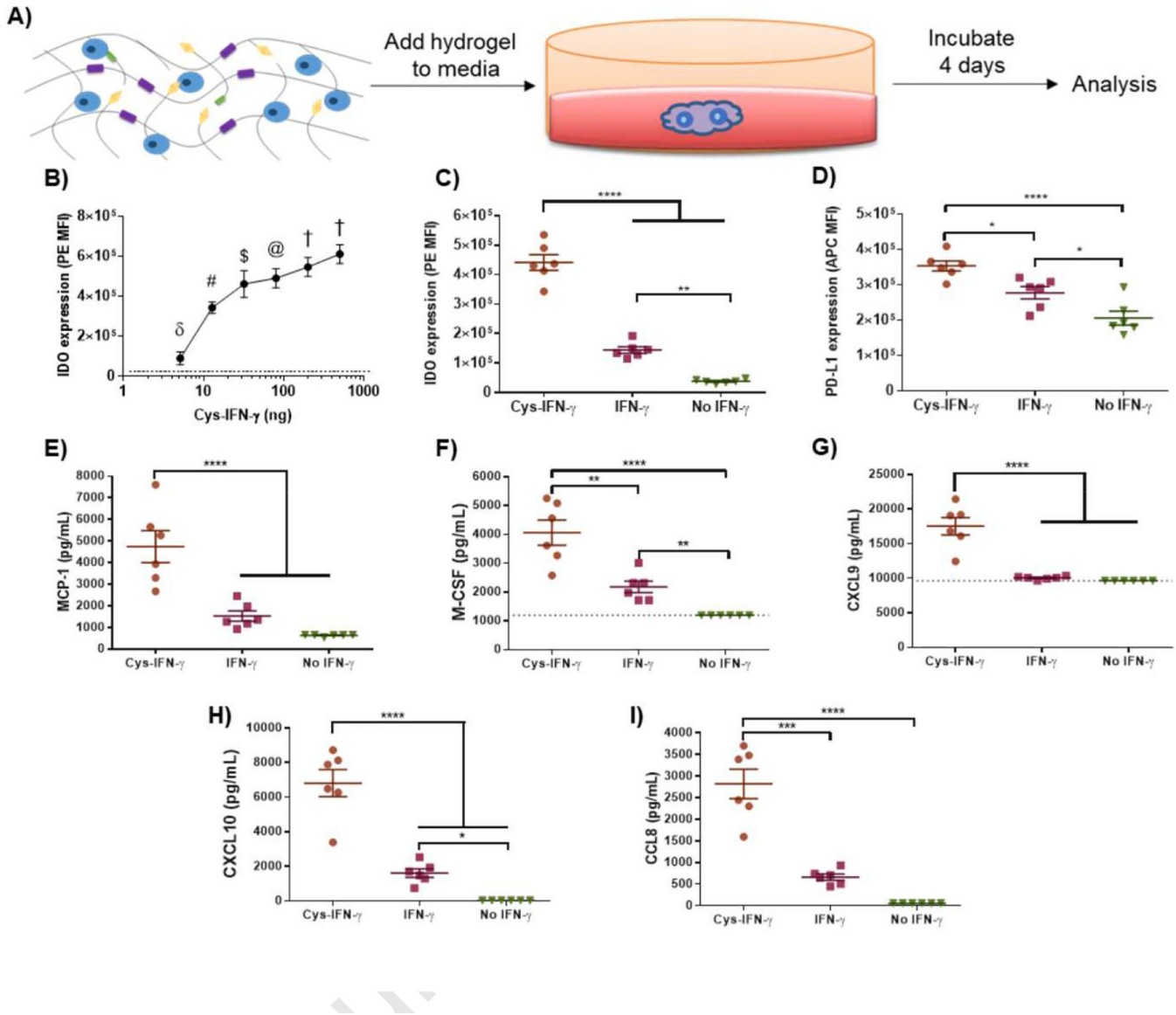

Figure 3.

Licensing of hMSCs encapsulated in cys-IFN-γ-tethered hydrogels. A) Schematic of experimental outline. hMSCs were encapsulated within hydrogels of different conditions and immunomodulatory properties analyzed. B) hMSCs were encapsulated in 6% PEG wt %, 20 μL hydrogels with differing doses of cys-IFN-γ. Following 4 days of culture, cells were subjected to flow cytometric analysis for IDO expression. Dotted line indicates level of IDO expression of 0 ng dose. N=3–5. δ $p<0.0001$ vs all conditions tested except 0 ng dose. # $p<0.05$ vs 32 ng and 80 ng doses, $p<0.001$ vs 200 ng dose, $p<0.0001$ vs 0, 5, and 500 ng dose. $ $p<0.001$ vs 500 ng dose, $p<0.0001$ vs 0 ng dose. @ $p<0.05$ vs 500 ng dose, $p<0.0001$ vs 0 ng dose. † $p<0.0001$ vs 0 ng dose. C,D) IDO and PD-L1 expression of hMSCs in hydrogels with cys-IFN-γ and IFN-γ. Following 4 days of culture, hMSCs in hydrogels with either cys-IFN-γ, IFN-γ or no IFN-γ were stained for C) IDO and D) PD-L1 and subjected to flow cytometric analysis. N=6. E-I) Cytokine analysis of conditioned media.

Conditioned media of hMSCs encapsulated in hydrogels with either cys-IFN-γ, IFN-γ or no IFN-γ was analyzed for E) MCP-1, F) MCSF, G) CXCL9, H) CXCL10, I) CCL8. N=6. Error bars ± SEM. One-way ANOVA * $p<0.05$, ** $p<0.01$, *** $p<0.001$, **** $p< 0.0001$.

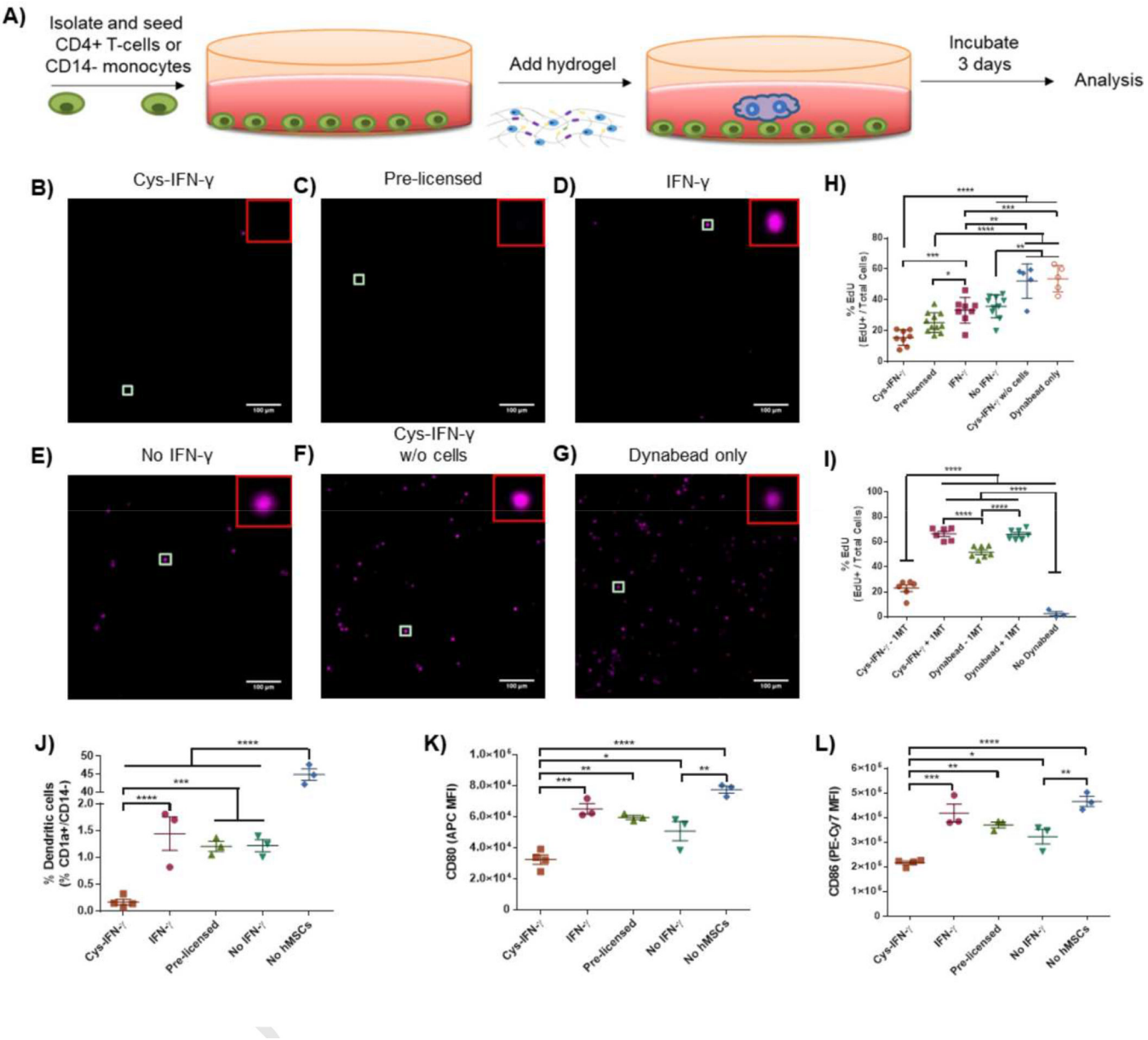

Figure 4.

hMSCs encapsulated in cys-IFN-γ hydrogels modulate immune cells. A) Schematic of experimental outline. hMSCs were encapsulated within hydrogels of different conditions and the effect on T-cells or monocytes analyzed. B-H) hMSCs encapsulated within cys-IFN-γ hydrogels significantly reduce activated CD4+ T-cell proliferation. B-G) Representative images of fluorescence microscopy images of proliferating T-cells stained for EdU, scale bar 100 μm. H) Untreated or pre-licensed hMSCs were encapsulated within cys-IFN-γ, IFN-γ or no IFN-γ hydrogels and co-cultured with activated CD4+ T-cells for 4 days. T-cell proliferation was assessed via EdU incorporation. Graph shows samples from two independent experiments. N= 5–8 separate wells with quantification of >100 T-cells per well. I) Quantification of proliferating T-cells with IDO inhibitor. N= 6–7 separate wells with quantification of >100 T-cells per well. J-L) hMSCs in cys-IFN-γ hydrogels inhibit

dendritic cell differentiation. J) Percentage of dendritic cells in monocyte culture after 7 days differentiation as defined by CD1a+/CD14- by means of FMO controls. Median fluorescence intensity for markers K) CD80 and L) CD86. N=3–4 separate wells with 20,000 cells analyzed per well. Error bars ± SEM. One-way ANOVA * $p<0.05$, ** $p<0.01$, *** $p<0.001$, **** $p<0.0001$.

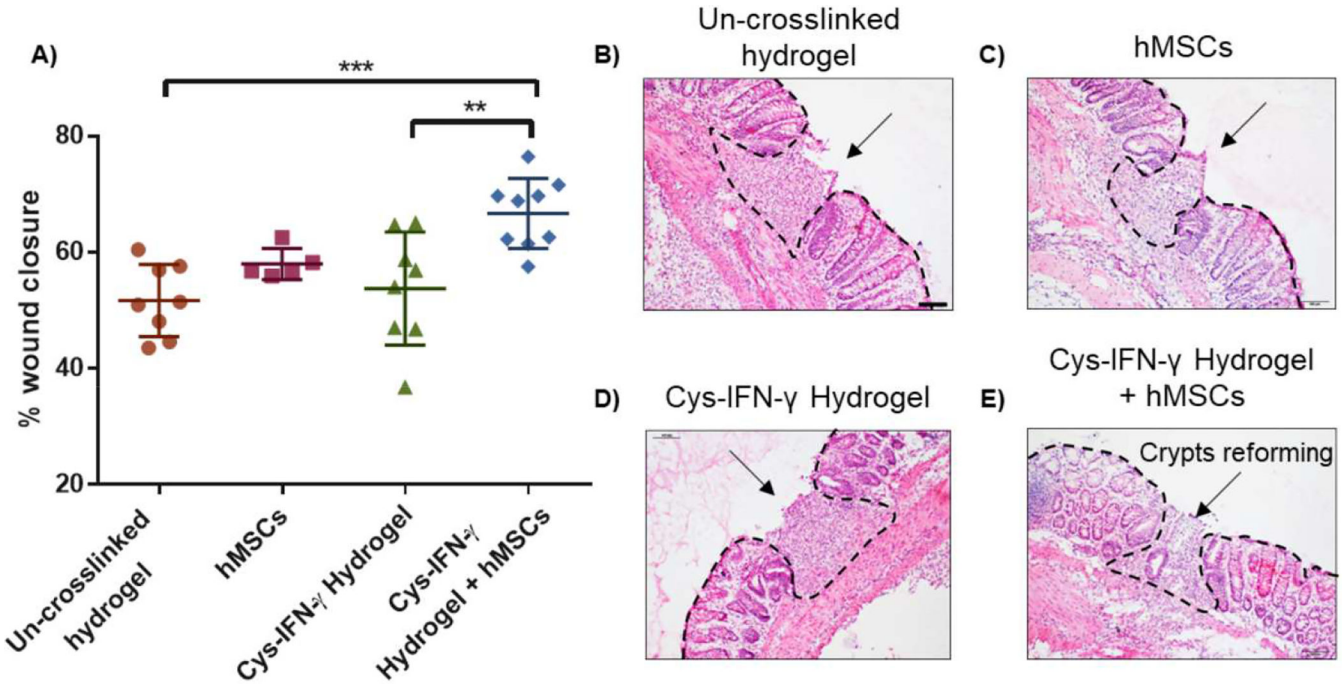

Figure 5.

hMSCs in cys-IFN-γ hydrogels repair colonic wounds in immunocompetent mice. A) Quantification of colonic wound closure at day 5 post-injury. B-E) H&E staining of colonic wounds at day 5 post-injury. Hashed line delineates tissue border to indicate wound. Arrow points to crypts reforming within repaired tissue. N=5–9 mice. Error bars ± SEM. One-way ANOVA ** $p<0.01$, *** $p<0.001$.